The integrative value of myocardial perfusion-function imaging with 13N-ammonia positron emission tomography

Juárez Orozco, Luis Eduardo

2

Imaging of cardiac and renal perfusion in a rat model with ^{13}N-ammonia microPET

Juárez-Orozco LE, Szymanski MK, Hillege HL, Kruizinga S, Noordzij W, Koole M, Tio RA, Alexanderson E, Dierckx RA, Slart RHJA

Published in the *International Journal of Cardiovascular Imaging*

2015 Jan;31(1):213-9

ABSTRACT

Purpose. Cardiac dysfunction leads to decreased organ perfusion. We aimed to measure cardiac and renal perfusion simultaneously with the use of ^{13}N-ammonia-microPET in a rat model.

Methods. Ten male Wistar rats underwent sham surgery (n=5) or permanent coronary artery ligation to induce myocardial infarction (Ml, n=5). Eleven weeks later a ^{13}N-ammonia-microPET scan was performed to image cardiac and renal perfusion.

Results. Cardiac perfusion was significantly reduced in MI group, directly correlated with ejection fraction and inversely correlated with MI size (r=0.89; p<0.001 and r=-0.86; p<0.001 respectively). Renal perfusion showed a notional 17% non-significant reduction in MI group when compared to sham (3.44±0.40 *vs* 4.12±0.48 ml/g/min). There was a trend towards greater reduction of perfusion in cortical than medullar region. Cortex perfusion was negatively correlated with histological changes.

Conclusion. ^{13}N-ammonia-microPET may be a potential tool for evaluation of cardiac and renal functional and perfusion changes in presence of cardiac dysfunction in rat models.

INTRODUCTION

Renal dysfunction is one of the most common co-morbidities in heart failure (HF) population. The co-existence of these entities results in worse prognosis (1). These observations revived interest in the pathophysiological interrelationship between heart and kidney. Although the exact mechanisms remain unclear, there are multiple factors known that play a role in this interaction (2). One of the pivotal mechanisms underlying this inter-organ relationship is hemodynamic changes – reduced cardiac output leading to reduced renal blood flow (RBF). Reduced RBF has been shown to be the main determinant of renal function (3), which is a strong prognostic factor in HF population (1). Not only is the total renal perfusion reduced in the presence of cardiac dysfunction, but also the differences between cortical and medullar renal blood flows have been observed (4). Moreover, different mechanisms underlie the regulation of blood flow in cortical and medullar regions (5). As a result, many vasoactive regulatory factors yield different effects on cortical and medullar blood flow. Since many of these factors, such as noradrenaline, angiotensin II and nitric oxide are known to play a role in cardiorenal syndrome and are being targeted by common treatment strategies, studies on regional renal perfusion in the presence of cardiac dysfunction might help understanding the pathophysiology behind this syndrome better and improve the treatment strategies.

Therefore, there is an impending need for a noninvasive, preclinical method for the evaluation of cardiac and renal kidney perfusion, which in turn could contribute to clarify the underlying dynamics of the cardiac and renal perfusion.

Positron emission tomography (PET) offers a promising, quantitative and minimally invasive alternative for measurements of organ perfusion. PET scans with ^{13}N-ammonia have been used to evaluate cardiac perfusion (6,7) as well as renal perfusion in humans (8) and large mammals (9,10). Since most of the experimental research on cardiorenal interaction is performed in rodents (11), we aimed to use ^{13}N-ammonia-microPET to investigate cardiac and renal perfusion in healthy rats and in a rat model based on myocardial infarction.

MATERIALS AND METHODS

Animals

The study was performed in 10 male Wistar rats (Harlan, The Netherlands). Animals were housed in groups under standard conditions at 12h light/dark cycle until they reached 12 weeks of age. All animals received standard diet and water ad libitum during the study. At 12 weeks of age rats were subjected to myocardial infarction (MI) (*n*=5) by permanent coronary artery ligation or sham surgery (*n*=5) as described before (12). Approximately 11 weeks after the surgery, the rats were subjected to micro-PET scanning. One week after PET scanning, the animals were sacrificed and heart and kidney tissue were collected for further histological analysis. All animal experiments were performed by licensed investigators in compliance with the Law on Animal Experiments of The Netherlands. The protocol was approved by the Committee on Animal Ethics of the University of Groningen.

Echocardiography

Echocardiographic measurements were obtained using a Vivid 7 (GE Healthcare) equipped with a 10-MHz transducer. Rats were anaesthetized using 1.5% isoflurane and were placed on a heating pad to maintain body temperature. Ejection fraction (EF) was calculated using the Teichholz method from short axis images obtained at mid-papillary level. Measurements were performed on 5 consecutive heart beats and presented as the mean of these values to avoid beat-to-beat variation.

Micro-PET data Acquisition

All rats were scanned while under 1.5% isoflurane anaesthesia and maintained in a fixed supine position. A heating pad was used to maintain a constant body temperature. ^{13}N-ammonia was injected intravenously into the penile vein. The radiotracer was administered as a 0.4 - 0.6 mL bolus, with an average dose of 55.2±5.0 MBq. A lutetium oxyorthosilicate detector-based tomograph (microPET FOCUS-220; Siemens Medical Solutions USA, Knoxville, TN) was used with a transaxial resolution of 1.35 mm in full-width at half-maximum. Camera acquisition was started simultaneously with injection of the tracer.

Data were acquired in a 128×128×95 matrix with a pixel width of 0.949 mm and a slice thickness of 0.796 mm. Coincidence window width was set at 6 ns. A 10-minute list-mode acquisition protocol was used for ^{13}N-ammonia imaging. Thereafter, a microCT scan was performed using a microCAT II system (Siemens Preclinical Solutions, Knoxville, TN, USA) using the same fixed bed with maintained stereotactic position. CT was used for co-registration of the micro-PET images.

Micro-PET data processing

PET data was reconstructed into 22 frames with a total of 10 min (12×5 sec, 8×30 sec, 2×150 sec) and corrected for detector sensitivity and dead time. PET images were corrected for scatter and reconstructed applying an interactive reconstruction algorithm. To correct for attenuation and scatter, an attenuation map was reconstructed from the transmission PET data of a ^{57}Co point source and a blank scan using MAP reconstructed transmission images and re-projected to the sinogram space to generate a correction file. Sinograms were corrected for attenuation and scatter and reconstructed using Ordered Subsets Expectation Maximization (4 iterations with 16 subsets) (OSEM 2D).

Blood flow maps were analyzed manually by ROI analysis using Inveon Research Workplace software (Siemens; USA). ROIs for cardiac perfusion evaluation were drawn on images in transverse planes on all images where the heart was visible including infarcted areas (Figure 1).

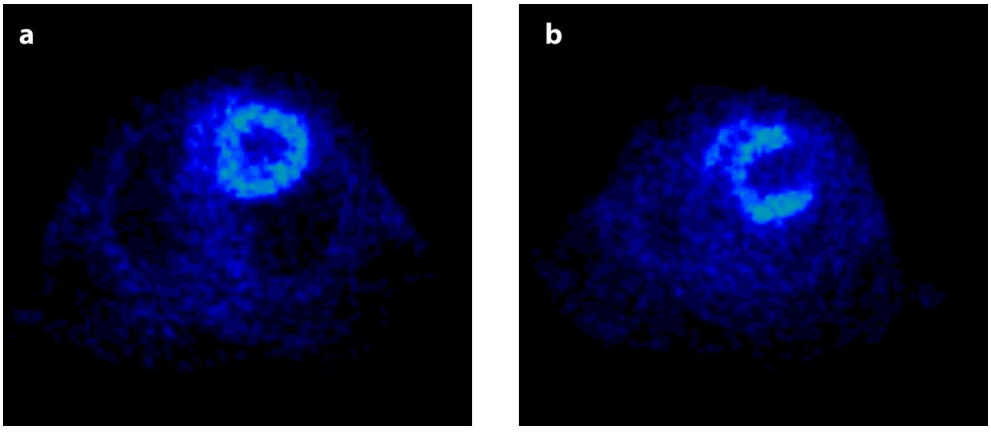

Figure 1. Analysis of cardiac perfusion for the sham group a), and MI group b). MI, myocardial infarction.

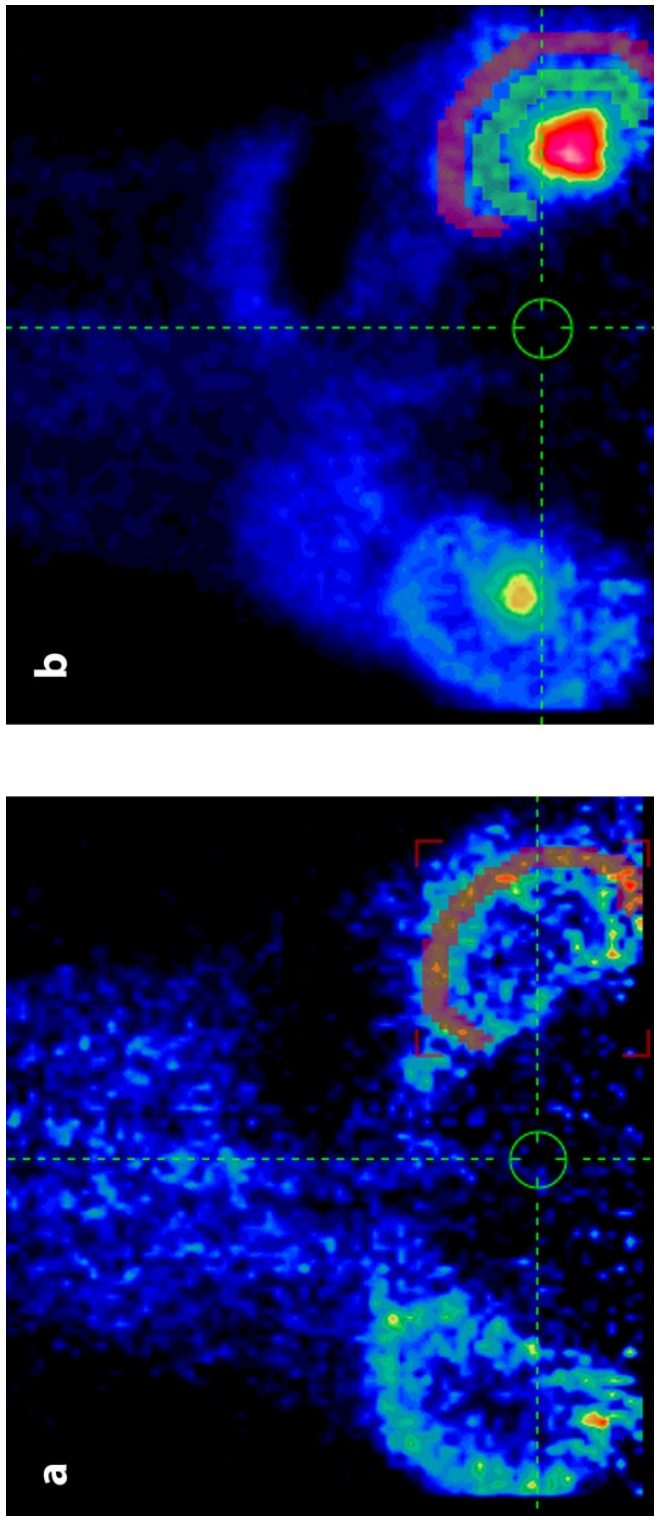

Figure 2. Analysis of regional renal blood flow. The placement of ROIs for perfusion analysis: a), selection of cortical region (in red); b), selection of medullar region (in blue/green). ROI, region of interest.

ROIs for renal perfusion evaluation were drawn on each kidney on 5 consecutive slices in coronal planes representing the middle section of the kidney. Firstly, the first 10 frames (5-60 seconds) were summed and ROIs for cortical region were drawn (excluding the medulla and collecting system [Figure 2a]). Subsequently all frames were summed and ROIs for medullary region were drawn (excluding collecting system and previously drawn cortical region [Figure 2b]).

Finally, ROIs were pooled to assess the mean RBF. Due to the partial tissue trapping of ^{13}N-ammonia, a two-compartment kinetic model was used as described before (10). Arterial input function was determined using ROIs placed in the left ventricle of the heart, excluding myocardial tissue. Organ perfusion is expressed in ml/g/min.

All scans were analyzed by two independent researchers blinded for the groups. The mean values of these analyses are reported.

Histology

After collection kidneys were longitudinal bisected, fixed in formaldehyde solution and subsequently embedded in paraffin. Sections of 4 μm were stained with periodic acid Schiff (PAS) and scored on presence and degree of focal glomerular sclerosis (FGS) as described before. FGS score was expressed in arbitrary units (AU) as described before (13). The sections were evaluated by an examiner who was blinded for the groups.

The heart was dissected, cooled in ice-cold saline for diastolic arrest. A midventricular slice was embedded in paraffin and subsequently stained with Sirius Red/ Fast Green. The infarct size was expressed as the mean of the inner and outer percentage of scar tissue to the inner and outer circumference of the left ventricle as described before (14).

Statistical analyses

Resulting data was explored for distribution and tested for normality. All data is presented as median ± standard error of the mean (SEM). A Mann-Whitney U test was used to compare the results between the independent groups; the test value, standardized statistic and significance are reported. Effect sizes according to the statistic test performed were calculated for the performed testing. Statistically significant differences were considered at a p–value < 0.05. All analyses were performed using SPSS software v.20.

RESULTS

At the moment of termination, mean body weight was similar in both groups of rats (458±19 *vs.* 459±20 g for MI and sham group respectively). Mean echocardiography-derived LVEF was 77.8±1.0% and 55.8±4.1% for sham and MI respectively, this difference was statistically significant (U=0; z=-2.619; p=0.008; r=-0.83). Mean histologically-derived infarct size was 32±8% in the MI group (p=0.008 *vs.* sham). There was a strong inverse correlation between LVEF and MI size in the whole study group (r=-0.89; p<0.001).

Cardiac perfusion measured with ^{13}N-ammonia micro-PET was reduced in MI group in comparison with the sham group (5.31±0.96 *vs.* 11.34±0.61 ml/g/min respectively) and this difference was statistically significant (U=0; z=-2.611; p=0.008), representing a large effect (r=0.85). A significant correlation between perfusion obtained with ^{13}N-ammonia micro-PET scan and both LVEF (r=0.89; p<0.001) and MI size (r=-0.86; p<0.001) was obtained.

Global and regional renal perfusion measurements with ^{13}N-ammonia micro-PET showed no statistically significant differences between the left and right kidney in any of the groups (Table 1).

Mean renal perfusion was decreased by 17% in MI group in comparison to sham and although the difference was not statistically significant (U=8; z=-0.940; p=0.42), it proved to document a medium effect size (r=-0.30). A similar pattern was seen with regard to regional perfusion. Both cortical and medullar perfusion values were lower in the MI group, however not significantly.

When compared to values obtained from the sham group, the reduction of the regional perfusion in the MI group seemed to be greater in cortex than in medulla (22% *vs.* 9% respectively), resulting in increased ratio between medulla and cortex perfusion (0.68±0.04 *vs.* 0.57±0.05), once more, even though this increase did not reach statistical significance (U=20; z=1.567; p=0.151), it proved a large effect size (r=0.5). There was no significant correlation between this ratio and any of the cardiac parameters.

The mean renal perfusion showed a positive correlation with cardiac perfusion (r=0.65; p=0.042) (Figure 3a), but not with LVEF (r=-0.59; p=0.12). There was a significant correlation between renal cortical and cardiac perfusion (r=0.73; p=0.016) (Figure 3b) and a trend towards correlation

with LVEF (r=0.62; p=0.058) and MI size (r=-0.60; p=0.070). There were no significant correlations or trends found for medullar perfusion with any of the cardiac parameters.

The histological analysis showed increased focal glomerulosclerosis in MI group (5.4±1.6 AU *vs* 1.0±0.4 AU for MI and sham, respectively (p=0.016) (Figure 4). There was a negative correlation between FGS and both global renal and cortical perfusion (r=-0.67; p=0.035; and r=-0.66; p=0.036 respectively)(Figure 2c and 2d).

Perfusion Variables (ml/g/min)	MI group (n=5)	Sham group (n=5)
Total kidney perfusion – mean	3.44 ± 0.40	4.12 ± 0.48
Left kidney	3.41 ± 0.42	4.06 ± 0.51
Right kidney	3.46 ± 0.39	4.17 ± 0.46
Right/left kidney ratio	1.02 ±0.02	1.05 ± 0.06
Cortex perfusion – mean	3.85 ± 0.37	4.92 ± 0.59
Left cortex	3.80 ± 0.39	4.88 ± 0.63
Right cortex	3.89 ± 0.36	4.97 ± 0.57
Right/left cortex ratio	1.03 ± 0.03	1.03 ± 0.06
Total medulla perfusion – mean	2.65 ± 0.36	2.90± 0.52
Left medulla	2.64 ± 0.35	2.98 ± 0.58
Right medulla	2.66 ± 0.38	2.82 ± 0.47
Right/left medulla ratio	1.00 ± 0.03	1.00 ± 0.09

Table 1. Regional and total kidney perfusion measurements. Data expressed in ml/g/min and presented as mean ± SEM.

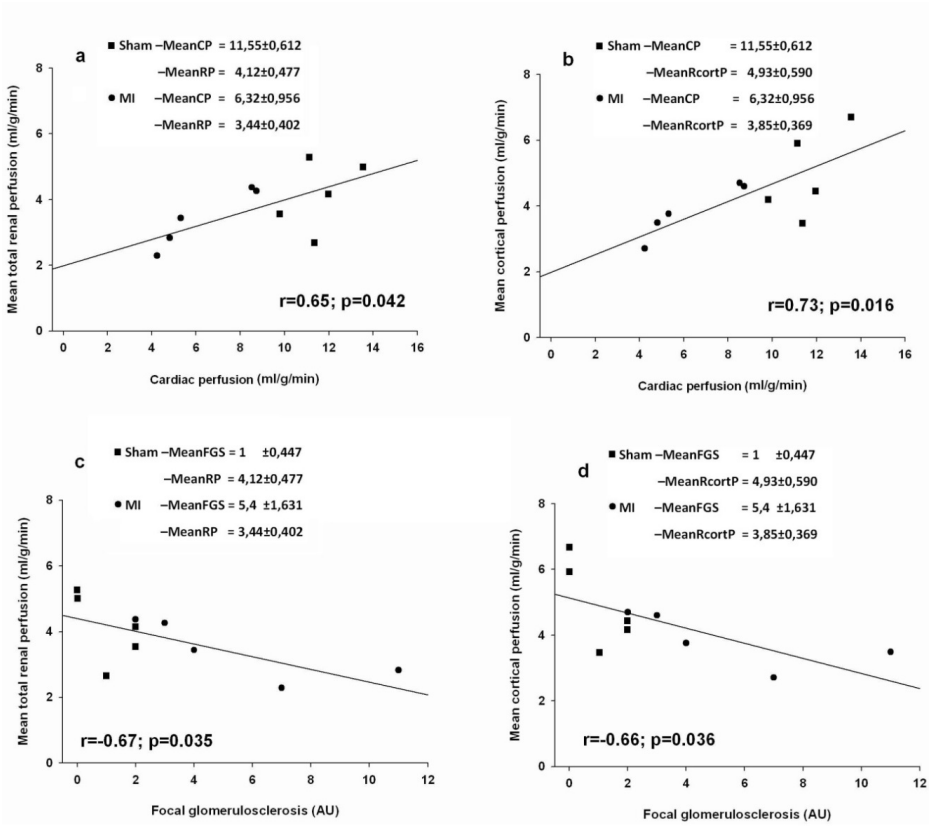

Figure 3. Correlations between total renal and cardiac perfusion (a), cortical and cardiac perfusion (b); total renal perfusion and focal glomerulosclerosis (c); cortical perfusion and focal glomerulosclerosis (d). AU; arbitrary units, CP; cardiac perfusion, RP; renal perfusion, RcortP; renal cortex perfusion, FGS; focal glomerulosclerosis.

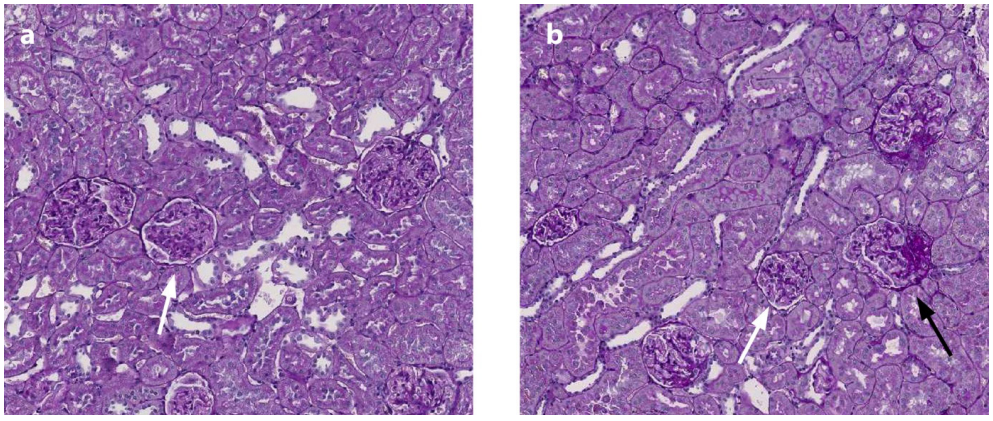

Figure 4. Representative microphotographs of cortex region. a) sham group b) MI group; white arrow indicating normal glomeruli and black arrow, sclerotic glomeruli. MI, myocardial infarction.

DISCUSSION

In the present study, we used ^{13}N-ammonia –microPET to evaluate the cardiac and renal blood flow in healthy rats and rats with myocardial infarction. We showed that experimental cardiac dysfunction leads to reduced cardiac perfusion and we found a trend towards reduction in renal perfusion. The latter reduction seemed to be higher in the cortical than medullar region of the kidney. Cardiac perfusion was significantly correlated with renal and cortical, but not with medullar perfusion. Interestingly, there was a negative correlation between cortical perfusion and the severity of histological changes in this region.

Myocardial infarction often leads to reduction in cardiac function and subsequently reduced peripheral organ perfusion. In our study, experimental MI led to decrease in cardiac perfusion. Cardiac perfusion was strongly correlated with infarct size and LVEF. There was a trend towards lowering of renal perfusion in animals with experimentally induced cardiac dysfunction. Notably, the calculated effect size (as an added value for standardized comparison of results across studies) revealed that this difference might represent a important medium sized effect given that it did not meet the expected statistical significance. The lack of significance might have resulted from small experimental groups and some variation in the induced infarct size. It has been shown that small infarcts do not lead to substantial reduction in cardiac function and cardiac output therefore renal perfusion might not be significantly affected. Nevertheless, we consider that this consideration should further encourage the extension of the experimental model in the proposed notion.

Not only is total renal perfusion affected in the presence of cardiac dysfunction, but it has also been shown, that cortical blood flow is markedly diminished, whereas medullary blood flow appears to be preserved (4). We were able to show this trend in the present analysis. Although the differences were not significant, cortical blood flow was reduced by 22% in comparison to 9% reduction in medullar perfusion, moreover, this finding was estimated as a large sized effect (r=0.5 and d=0.99), which supports interest in further examination of the phenomenon.

The significant correlation between cardiac and cortical but not medullar perfusion found in our study supports the observations of different regulation mechanisms of regional renal blood flow (5). Whereas

in the medullar region vasodilation occurs to preserve the blood flow (15), the activated renin-angiotensin-system leads to vasoconstriction in the cortical region (16). Increased angiotensin II levels lead to glomerular hyperperfusion and increased filtration fraction and preservation of kidney function. However, chronic high angiotensin II concentrations cause glomerular matrix accumulation and progression of glomerulosclerosis. Activation of regulatory systems and preferential vasoconstriction of renal cortical vessels may also contribute to the increased sodium retention and subsequently increased venous pressures with oedema formation (16). This leads to higher pressures in the kidney and hypoxia, which may cause further histological changes and decrease of kidney function (17). In the present study we showed increased glomerulosclerosis in MI group and a significant correlation between severity of glomerulosclerosis and cortical perfusion. Again, this correlation was not found for the medullar perfusion which provides additional evidence for different regulatory mechanisms.

In the present study, we used ^{13}N-ammonia -microPET for cardiac and renal perfusion measurements in rats. The advantage of this approach is the possibility of simultaneous measurement of perfusion of these two organs. Recently, we have shown that ECG-gated ^{13}N-ammonia -microPET can also be used for estimation of cardiac volumes and function, which extends the possibilities of this method (18). PET imaging furthermore allows repetitive imaging due to its non-invasive character whereas cardiac perfusion measurements have been described before (19). The technique we used might offer a promising, quantitative, consistent and minimally invasive alternative for measurements of regional RBF (20). The accuracy of RBF measurements with the use of PET depends on the tracer. In this study we used the perfusion tracer ^{13}N-ammonia, which has been described and validated by comparison to microspheres before (10). Renal retention of ^{13}N and its relative long half-life compared to another perfusion tracer ^{15}O-water allows extended image acquisition periods. Also the shorter range of the ^{13}N positron compared with ^{15}O-water is attractive. This leads to better quality of acquired images. Because of the tracer kinetics, this method requires a two-compartment model. Since ^{13}N-ammonia is rapidly metabolized, it has been argued that the values of arterial input should be corrected for ^{13}N-ammonia metabolites in blood. An analysis by Chen showed that there is only little contamination, which leads to limited underestimation of the results and therefore the correction is not necessary (10).

Due to the complicated structure of the kidney, systematic errors due to finite spatial resolution and partial-volume effects might occur. This might lead to underestimation of cortical flow and thus the ability to show subtle differences in regional blood flow might be limited. It can also not be excluded that within the cortical ROIs an unknown part of medullar region was included and vice-versa. Although the maximal size of ROIs did correspond with the size of the cortex region found in histological studies and the PET flow maps provided relatively sharp boundaries of cortical region, the accuracy of the ROIs location should be interpreted with some caution.

LIMITATIONS

Our study is limited by the small size of experimental groups. Variation in infarct size between animals in MI group was seen, which in some animals might have resulted in only a slight reduction of cardiac function and therefore limited effects on renal perfusion. Additionally, the lack of significance in the correlation between LVEF and infarct size with cortical renal perfusion may have resulted from the relatively short duration of the post-infarction follow-up. This notion could be supported by the finding of an important effect size concerning the renal perfusion ratios. We did not perform simultaneous microsphere blood flow measurements to compare results; however, the used protocol has been described and validated in literature before and resulting trend suggests further research must be addressed.

CONCLUSION

Micro-PET using ^{13}N-ammonia might serve as a useful non-invasive tool for measurements of cardiac and regional renal perfusion in small animal models. The possibility to evaluate regional renal perfusion in rodents might help to understand the changes occurring in kidneys in the presence of cardiac dysfunction. The use of ^{13}N-ammonia allows simultaneous assessment of cardiac and renal perfusion in rodents. This all may contribute to better understanding of the cardiorenal syndrome.

REFERENCES

1. Hillege HL, Girbes AR, de Kam PJ, Boomsma F, de Zeeuw D, Charlesworth A, et al. *Renal function, neurohormonal activation, and survival in patients with chronic heart failure*. Circulation. 2000 Jul 11;102(2):203–10.
2. Ronco C, Haapio M, House AA, Anavekar N, Bellomo R. *Cardiorenal syndrome*. J Am Coll Cardiol. 2008 Nov 4;52(19):1527–39.
3. Smilde TDJ, Damman K, van der Harst P, Navis G, Daan Westenbrink B, Voors A a., *et al*. Differential associations between renal function and "modifiable" risk factors in patients with chronic heart failure. Clin Res Cardiol. 2009;98(2):121–9.
4. Kilcoyne MM, Schmidt DH, Cannon PJ. *Intrarenal blood flow in congestive heart failure*. Circulation. 1973 Apr;47(4):786–97.
5. Evans RG, Eppel GA, Anderson WP, Denton KM. *Mechanisms underlying the differential control of blood flow in the renal medulla and cortex*. J Hypertens. 2004 Aug;22(8):1439–51.
6. Kudo T, Fukuchi K, Annala AJ, Chatziioannou AF, Allada V, Dahlbom M, et al. *Noninvasive measurement of myocardial activity concentrations and perfusion defect sizes in rats with a new small-animal positron emission tomograph*. Circulation. 2002 Jul 2;106(1):118–23.
7. Tio RA, Dabeshlim A, Siebelink H-MJ, de Sutter J, Hillege HL, Zeebregts CJ, et al. *Comparison between the prognostic value of left ventricular function and myocardial perfusion reserve in patients with ischemic heart disease*. J Nucl Med. 2009 Feb;50(2):214–9.
8. Nitzsche EU, Choi Y, Killion D, Hoh CK, Hawkins RA, Rosenthal JT, et al. *Quantification and parametric imaging of renal cortical blood flow in vivo based on Patlak graphical analysis*. Kidney Int. 1993 Nov;44(5):985–96.
9. Killion D, Nitzsche E, Choi Y, Schelbert H, Rosenthal JT. *Positron emission tomography: a new method for determination of renal function*. J Urol. 1993 Sep;150(3):1064–8.
10. Chen BC, Germano G, Huang SC, Hawkins RA, Hansen HW, Robert MJ, et al. *A new noninvasive quantification of renal blood flow with N-13 ammonia, dynamic positron emission tomography, and a two-compartment model*. J Am Soc Nephrol. 1992 Dec;3(6):1295–306.
11. Szymanski MK, De Boer R a., *Navis GJ, Van Gilst WH, Hillege HL*. Animal models of cardiorenal syndrome: A review. Heart Fail Rev. 2012;17(3):411–20.
12. Westenbrink BD, Lipsic E, van der Meer P, van der Harst P, Oeseburg H, Du Marchie Sarvaas GJ, et al. *Erythropoietin improves cardiac function through endothelial progenitor cell and vascular endothelial growth factor mediated neovascularization*. Eur Heart J. 2007;28:2018–27.
13. Ulu N, Schoemaker RG, Henning RH, Buikema H, Teerlink T, Zijlstra FJ, et al. *Proteinuria-associated endothelial dysfunction is strain dependent*. Am J Nephrol. 2009;30(3):209–17.
14. Van Kerckhoven R, van Veghel R, Saxena PR, Schoemaker RG. *Pharmacological therapy can increase capillary density in post-infarction remodeled rat hearts*. Cardiovasc Res. 2004 Feb 15;61(3):620–9.
15. Abassi Z, Gurbanov K, Rubinstein I, Better OS, Hoffman a, Winaver J. *Regulation of intrarenal blood flow in experimental heart failure: role of endothelin and nitric oxide*. Am J Physiol. 1998;274:F766–74.
16. Ichikawa I, Pfeffer JM, Pfeffer M a., *Hostetter TH, Brenner BM*. Role of angiotensin II in the altered renal function of congestive heart failure. Circ Res. 1984 Nov;55(5):669–75.
17. Norman JT, Fine LG. *Intrarenal oxygenation in chronic renal failure*. Clin Exp Pharmacol Physiol. 2006 Oct;33(10):989–96.
18. Szymanski MK, Kruizinga S, Tio RA, Willemsen ATM, Schäfers MA, Stegger L, et al. *Use of gated 13N-NH3 micro-PET to examine left ventricular function in rats*. Nucl Med Biol. 2012 Jul;39(5):724–9.
19. Aukland K. *Methods for measuring renal blood flow: total flow and regional distribution*. Annu Rev Physiol. 1980;42(17):543–55.
20. Green MA, Hutchins GD. *Positron emission tomography (PET) assessment of renal perfusion*. Semin Nephrol. 2011 May;31(3):291–9.